A COMPREHENSIVE DESIGN APPROACH FOR A THREE-PHASE HIGH-FREQUENCY SINGLE-SWITCH DISCONTINUOUS-MODE BOOST POWER FACTOR CORRECTOR BASED ON ANALYTICALLY DERIVED NORMALIZED CONVERTER COMPONENT RATINGS

JOHANN W. KOLAR, HANS ERTL, FRANZ C. ZACH

Technical University Vienna, Power Electronics Section, Gusshausstrasse 27,
A-1040 Vienna, AUSTRIA

Phone: (int)43-1-58801-3886   Fax: (int)43-1-5052666

Abstract

In this paper the peak, mean and rms values of the component currents of a three-phase single-switch discontinuous inductor current mode boost rectifier are calculated analytically. The values are given in rated form in dependency on the output power and on the ratio of output voltage to the amplitude of the mains voltage. Furthermore, the influence of the voltage transfer ratio on the shape of the mains currents and on the power factor of the system is analysed. The theoretical analysis is verified by digital simulation and a good consistency is achieved. Finally, the approach of the converter dimensioning based on the graphical representation of the calculation results is described and illustrated using a specific example.

1 Introduction

Based on the standards (IEC 555-2) and recommendations (IEEE-519) aiming for a reduction of the effects on the mains and on the often given requirement for high power density of power electronic systems the development of self-commutated pulse rectifier systems with high operating frequency gains increasing importance [1], [2], [3].

In [4], which constitutes a major milestone of the development of unidirectional three-phase pulse rectifier systems, a single-switch discontinuous inductor current mode (DICM) boost rectifier (cf. Fig.1) is introduced which is characterized by:

- approximately sinusoidal input currents,
- resistive fundamental mains behavior,
- controllability of the output voltage u_O (being higher than the peak value of the mains line-to-line voltage).

In connection with the

- very simple structure of the power circuit and the control circuit

this system is of special interest for a hardware realization in the area of electrical drives and for process technology power supplies. E.g., the application of this system for feeding the DC voltage link of a PWM inverter makes possible

- the reduction of the filtering effort for limitation of the effects on the mains,

- the control of the DC link voltage to a constant value, independent of the mains voltage and, therefore,
- the maximum utilisation of the rated power of the PWM inverter, or of
- a matching to different mains voltage nominal values.

This can be achieved with a relatively small additional effort as compared to (uncontrolled) mains-commutated bridge rectification. The simple circuit structure of the proposed converter is paid for, however, by relatively high peak currents and voltages. This makes necessary an exact analysis of the stress on the components for defining the application region of the circuit.

Due to the single-phase equivalent circuit assumed in [4], the analysis of the operating behavior of the system given there is only valid with sufficient accuracy for high output voltage values as compared to the input voltage. Therefore, the guidelines given in [4] cannot be applied for dimensioning the system components and for the calculation of the system costs and the manufacturing costs for the application of the system in the European 380 V-mains (DC output voltage typically < 820 V).

An analytical calculation of the component stresses and of the characteristic system parameters being valid with high accuracy in the entire output voltage region is the topic of this paper. After a short description of the basic operating principle of the circuit (given in section 2), section 3 discusses the analysis method which is applied in section 4 for the calculation of the component stresses in dependency on the output power. The calculation of the mains current shape and of the mains power factor is given in section 5. Finally, in section 6 the approach for dimensioning the system is described and illustrated by a numerical example.

2 Principle of Operation

The control of the system shown in Fig.1 is performed in the stationary case by a pulse frequency f_P and an on-time of the power transistor T being constant within the mains fundamental period [4]. A synchronization of f_P to the mains frequency f_N can be omitted for $f_P \gg f_N$. According to the low-pass characteristic of the mains filter L_N, C_N the mains voltage can be thought as lying directly at the filter output side. Regarding the mains phase voltages (being approximately constant within the pulse period) we will assume $u_{N,R} > 0$, $u_{N,T} \leq u_{N,S} \leq 0$ in the following. (This is valid within an interval of $\pi/6$ of the fundamental period, cf. Fig.2, (a)). Under the assumption of a symmetric, purely sinusoidal three-phase mains voltage the system behavior within the
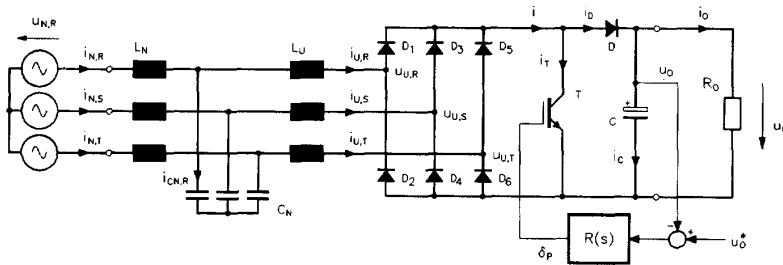
Fig.1: Structure of the power circuit and the control circuit of a three-phase single-switch discontinuous inductor current mode boost rectifier; filtering of the high-frequency spectral components of the discontinuous input currents $i_{U,(RST)}$ of the three-phase diode bridge by a mains filter L_N, C_N (shown simplified as single-stage filter). The feeding mains is replaced by a Y-connection of ideal voltage sources $u_{N,(RST)}$; the control of the power transistor T is performed with constant pulse frequency f_P and with a relative on-time (duty-cycle) δ_P being constant within the fundamental period and given by an output voltage controller.
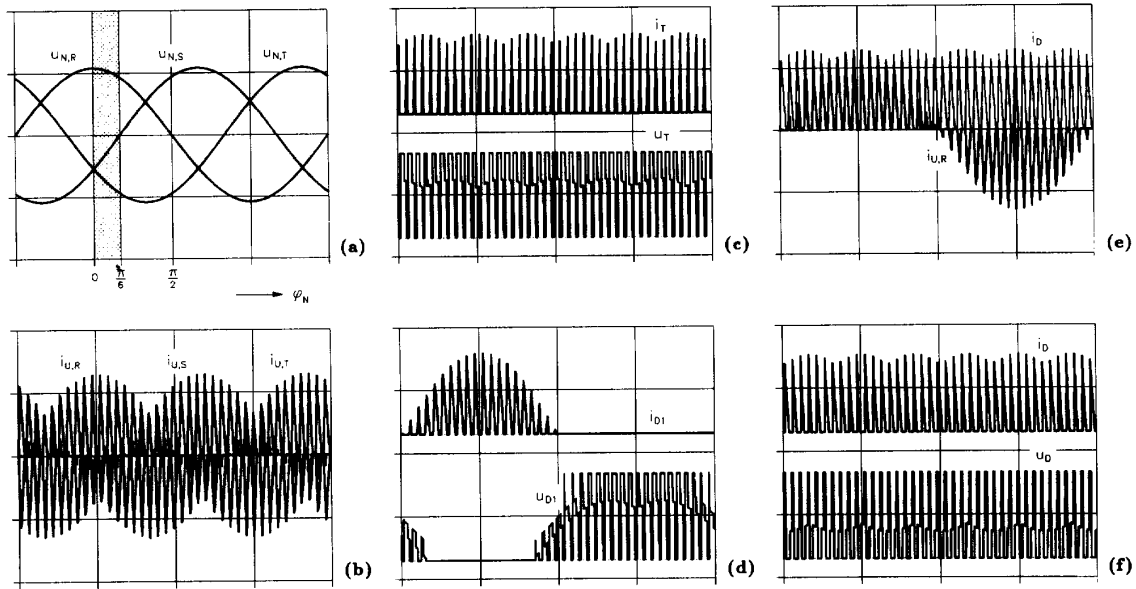
Fig.2: Digital simulation of a three-phase discontinuous-mode boost rectifier (without mains filter) being operated with constant pulse frequency f_P. For a clear representation of the system behavior, a low pulse frequency has been assumed; on-time $t_{\mu,1}$ of T constant within the fundamental period; (a): mains phase voltages $u_{N,(RST)}$; (b): input phase currents $i_{U,(RST)}$; (c): transistor current i_T and transistor voltage u_T; (d): current i_{D1} and blocking voltage u_{D1} of diode D_1 of the three-phase bridge rectifier; (e): output current i of the three-phase diode bridge and phase current $i_{U,R}$; (f): diode current i_D feeding the DC link and diode blocking voltage u_D; scaling: (a): 300V/div; (b)–(f): 25A/div or 600V/div, respectively; parameters: $U_O = 820$V, $P_O = 5.5$kW, $L_U = 1.25$mH $T_N = 20$ms, $f_P = 1/T_P = 1.95$kHz.

entire fundamental period is defined therefore, due to the phase-symmetric converter structure. The DC output voltage u_O should be sufficiently higher than the peak value of the line-to-line mains voltage. (The output voltage has a lower limit of $\sqrt{3}\,\hat{U}_N$, according to the boost-converter structure.)

Before turning on transistor T, we have $i_{U,R} = i_{U,S} = i_{U,T} = 0$ (system operating in discontinuous mode). T is switched on at instant $t_\mu = 0$. t_μ denotes a *local* time being counted within the considered pulse period. The rate of rise of the phase currents resulting due to the DC-side short circuit of the diode bridge is defined by the magnitudes of the phase voltages and by the inductances L_U. After turning off T in $t_{\mu,1}$ as given by the output voltage controller, the demagnetization of the inductances L_U via diode D into the capacitor C which buffers the output voltage is performed. There, only within the first part $t_\mu \in [t_{\mu,1}, t_{\mu,2}]$ of the demagnetization interval all three phases conduct current, however (cf. Fig.3). At $t_{\mu,2}$ that phase current becomes 0 which shows the smallest magnitude at $t_\mu = t_{\mu,1}$ (in the case at hand, $i_{U,S}$). The following second demagnetization interval (demagnetization of the two remaining phases R and T which conduct current of equal magnitude, but of opposite direction) is finished at $t_\mu = t_{\mu,3}$. Therefore, proper dimensioning has to guarantee $t_{\mu,3} \le T_P$ for discontinuous mode.

Remark: As the considerations given show clearly, the operating behavior of a three-phase diode bridge which defines the current shape within the demagnetization interval basically *cannot* be described by (decoupled) single-phase bridge circuits. If the operating behavior of the system is analysed using a single-phase equivalent circuit, only the current shape within the turn-on interval of T is described correctly. Therefore, the calculations given in [4] can only be used as a coarse approximation for the determination of the component stresses in the case of a demagnetization period being short as compared to the on-time of T or, for $U_O \gg \sqrt{3}\,U_O$, respectively.

Figure 2 shows the current and voltage shapes of a three-phase boost rectifier operated with low pulse frequency, as determined by digital simulation. The discontinuous input phase currents $i_{U,(RST)}$ follow envelopes which are proportional to the respective phase voltages $u_{N,(RST)}$. Via filtering of the switching frequency spectral components using a mains filter L_N, C_N connected in series (cf. Fig.1) we obtain an approximately resistive loading of the mains as related to the fundamental of the mains currents $i_{N,(RST)}$. One has to point out that, due to the on-time of T being constant within the

fundamental period, the current control is performed directly by the mains voltage and not, e.g., by a sinusoidal variation of the duty ratio.

3 System Analysis

3.1 Assumptions

For limitation on the essentials, the analysis of the converter system is based on the following assumptions:

- purely sinusoidal, symmetric mains voltage system $u_{N,(RST)}$,
- ideal filtering of the pulse-frequency spectral components of the converter input currents $i_{U,(RST)}$ by a mains filter L_N, C_N,
- negligible ripple voltage across the filter capacitors C_N,
- negligible fundamental voltage drops across the filtering inductances L_N as compared to the amplitude $\hat{U}_N$ of the voltage of the supplying mains (the filter capacitor voltage is assumed as being impressed and set equal to the mains voltage),
- constant output voltage U_O,
- constant load current I_O,
- $f_P > 200 f_N$ or $T_P \ll T_N$ (mains phase voltages approximately constant within a pulse period),
- ideal system components (especially: negligible system losses, switching times, etc.).

The assumption of a pulse frequency being sufficiently higher than the mains frequency is of special importance there. As described in the following section, this assumption makes possible a calculation of very exact analytical approximations of characteristic parameters being relevant for the dimensioning.

3.2 Analysis Method

As a basis for dimensioning of the active and passive components we have to calculate the mean and rms values of the device currents i; besides their peak
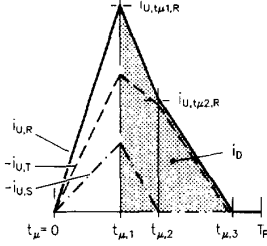
Fig.3: Time shape of the converter input currents $i_{U,(RST)}$ and of the output diode current i_D marked by the dotted area within a pulse period $t_\mu \in [0, T_P]$ for $u_{N,R} > 0$, $u_{N,T} \leq u_{N,S} \leq 0$ (valid within the angle interval $\varphi_N \in [0, \frac{\pi}{6}]$, cf. Fig.2, (a)); t_μ denotes a local time being counted within the pulse period; $t_\mu = t_{\mu,1}$: turn-off instant of T; the position of the considered pulse interval within the fundamental period is set by the global time t or by the phase angle $\varphi_N = \omega_N t$; parameter: $M = 1.5$.

values. There, the determination of the averaged (related to the fundamental period) characteristic parameters of the currents has to be performed via the summation of the contributions of the single pulse intervals and is not possible in analytically closed form, therefore.

As shown, e.g., in [5] and [6], one can now replace (for a pulse frequency being high as compared to the fundamental frequency) the summation according to

$$I_{i,avg} = \frac{6}{\pi} \int_0^{\frac{\pi}{6}} \{ \frac{1}{T_P} \int_0^{T_P} i_i(\varphi_N, t_\mu) \, dt_\mu \} \, d\varphi_N \quad (1)$$

$$I_{i,rms}^2 = \frac{6}{\pi} \int_0^{\frac{\pi}{6}} \{ \frac{1}{T_P} \int_0^{T_P} i_i^2(\varphi_N, t_\mu) \, dt_\mu \} \, d\varphi_N \quad (2)$$

by an integration. There, φ_N defines the position of a pulse interval within the fundamental period. The relation to the (global) time t is given by the relation

$$\varphi_N = \omega_N t \,. \quad (3)$$

As explained in section 2, the consideration of the symmetry relations of a three-phase system allows the limitation of the integration interval to a $\pi/6$ wide section of the fundamental period.

With this the characteristic values of the currents can be calculated directly and analytically. One has to point out that contrary to a numerical calculation (whose validity always is restricted to discrete parameter values) the analytical calculation allows an immediate statement concerning the influence of the system parameters (input voltage, output voltage, output power, pulse frequency etc.) on the dimensioning of the converter.

In connection with a minimization of size and weight of the magnetic components we have to aim in a practical realisation, by all means, at a pulse frequency of the converter being much higher than the mains frequency. Due to the discontinuous mode a stress on the transistor T by reverse recovery currents of the output diode D is avoided; in this case a pulse frequency $f_p \geq 200 f_N$ seems to be obtainable. As a check of the calculation based on the assumptions made in section 3.1 shows (performed by digital simulation), the derivations of the analytically calculated approximations from the exact (simulated) values remain below 2% there. Therefore, the calculation results given in sections 4, 5 and 6 can be used directly as basis for dimensioning of the components.

3.3 Normalization

For a simplification and a wide applicability of the relations derived in this paper, the results are represented in rated form:

$$t_{\mu,i,r} = \frac{1}{T_P} t_{\mu,i} \quad u_{i,r} = \frac{1}{U_O} u_i \quad i_{i,r} = \frac{1}{I_n} i_i \quad p_{i,r} = \frac{1}{P_n} p_i \,. \quad (4)$$

Into the base quantities of the normalisation

$$I_n = \frac{2}{3} U_O \frac{T_P}{L_U} \qquad P_n = \frac{2}{3} U_O^2 \frac{T_P}{L_U} \quad (5)$$

the parameters are included which directly influence the system behavior, namely T_P, L_U and U_O. The normalization is performed related to the DC output voltage, because with this the normalization basis remains unchanged for varying mains voltage conditions (caused by the tolerance band of the mains voltage or different nominal levels of the mains voltage).

3.4 Definitions

For characterizing the voltage transfer ratio of the system the ratio between DC output voltage to the peak value of the mains line-to-line voltage is applied:

$$M = \frac{U_O}{\sqrt{3} \hat{U}_N} \qquad M \geq 1 \,. \quad (6)$$

Due to the boost converter structure the output voltage range has a lower limit given by the peak value $\sqrt{3}\,\hat{U}_N$ of the mains line-to-line voltage. For the relative on-time of the transistor T (duty cycle) we define:

$$\delta_P = \frac{t_{\mu,1}}{T_P} \,. \quad (7)$$

The sum of the on-time of T and the maximum duration of the demagnetisation interval (cf. Eq.(15)), defining the transition into the continuous mode, is determined via

$$\delta = \frac{T}{T_P} \,. \quad (8)$$

For discontinuous mode we have to guarantee $\delta \geq 1$.

4 Basic Equations

According to Eqs.(1,2) the calculation of the current stresses on the components has to be based on the current shape within a pulse period $t_\mu \in [0, T_P]$. As can be seen immediately from the description of the operating behavior in section 2 and as illustrated in **Fig.3** using the example of the output diode current, the local shape of all device currents can be derived directly from the shape of the converter input currents $i_{U,(RST)}$. Furthermore, the mathematical description of the current shape also yields a statement about that maximum on-time of T or about the maximum output power for which the limit to the discontinuous mode is reached.

The calculation of the input currents is performed for time-constant pulse frequency f_P and for a local on-time $t_{\mu,1}$ of T being constant over the fundamental period. Furthermore, exclusively the discontinuous mode is assumed.

Remark: For a partly discontinuous and continuous system operation a simple analytical formulation is not possible. Due to the occurrence of low-frequency mains current harmonics and a phase shift between mains current and mains voltage fundamentals [7] such modes of operation have no practical significance, however.

As already described in section 2, for the assumption of a symmetric mains voltage system

$$u_{N,R} = \hat{U}_N \cos(\varphi_N)$$

$$u_{N,S} = \hat{U}_N \cos(\varphi_N - \frac{2\pi}{3})$$

$$u_{N,S} = \hat{U}_N \cos(\varphi_N + \frac{2\pi}{3}) \quad (9)$$

the calculation can be limited to the interval $\varphi_N \in [0, \frac{\pi}{6}]$ (cf. Fig.2). Due to the assumption of phase voltages being constant within a pulse period the phase currents show piece-wise linear shapes (cf. Fig.3); for the current values and time intervals $(\Delta t_{\mu,ji} = t_{\mu,j} - t_{\mu,i})$ defining the time behavior, there follows after a short calculation:

$$t_\mu = t_{\mu,1}: \qquad i_{U,t\mu1,R,r} = \frac{\sqrt{3}}{2} \delta_P M^{-1} \cos(\varphi_N)$$

$$i_{U,t\mu1,S,r} = \frac{\sqrt{3}}{2} \delta_P M^{-1} \cos(\varphi_N - \frac{2\pi}{3})$$

$$i_{U,t\mu1,T,r} = \frac{\sqrt{3}}{2} \delta_P M^{-1} \cos(\varphi_N + \frac{2\pi}{3}) \quad (10)$$

$$t_\mu = t_{\mu,2}: \qquad i_{U,t\mu2,R,r} = \frac{3}{2} \delta_P M^{-1} \frac{\sin(\varphi_N)}{1 + \sqrt{3} M^{-1} \sin(\varphi_N - \frac{\pi}{6})} \quad (11)$$
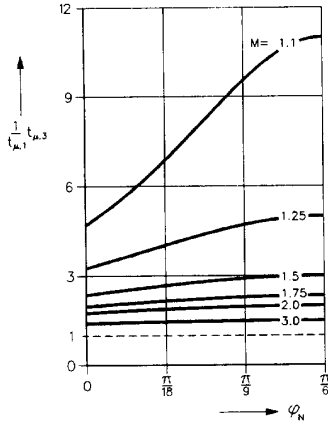
Fig.4: Local on-time $t_{\mu,3}$ (cf. Fig.3) of the input diode bridge related to the turn-on time $t_{\mu,1}$ of the power transistor T in dependency on the position φ_N of the considered pulse interval within the fundamental period (cf. Eq.(13)); parameter: voltage transfer ratio M.

$$t_\mu = t_{\mu,2}: \qquad i_{U,t\mu2,S,r} = 0$$

$$i_{U,t\mu2,T,r} = -i_{U,t_\mu2,R,r} \tag{11}$$

$$\Delta t_{\mu,21,r} = \sqrt{3}\,\delta_P M^{-1}\,\frac{\sin(\frac{\pi}{6} - \varphi_N)}{1 + \sqrt{3}M^{-1}\sin(\varphi_N - \frac{\pi}{6})} \tag{12}$$

$$\Delta t_{\mu,32,r} = 2\,\delta_P M^{-1}\,\frac{\sin(\varphi_N)}{(1 + \sqrt{3}M^{-1}\sin(\varphi_N - \frac{\pi}{6}))(1 - M^{-1}\cos(\varphi_N - \frac{\pi}{6}))}.$$

Regarding a more detailed derivation of the relations given here, cf. [8]. For the dependency of the local current flow interval of the input bridge rectifier on the position φ_N of the pulse interval and on the voltage transfer ratio M there follows with Eq.(12):

$$t_{\mu,3} = t_{\mu,1}\frac{1}{1 - M^{-1}\cos(\varphi_N - \frac{\pi}{6})} \tag{13}$$

(cf. **Fig.4**). Therefore, the maximum current flow interval determing the transition into the continuous mode is given by:

$$T = t_{\mu,3,max} = t_{\mu,3}\big|_{\varphi_N=\frac{\pi}{6}} = t_{\mu,1}\frac{1}{1 - M^{-1}}. \tag{14}$$

Due to the constant on-time $t_{\mu,1}$ the maximum conduction interval is determined by the maximum demagnetisation interval. One has to point out that the maximum value occurs at the maxima of the line-to-line mains voltages (for $\varphi_N \in [0, \frac{\pi}{6}]$ we have the maximum of the line-to-line mains voltage $u_{N,RT} = u_{N,R} - u_{N,T}$ at $\varphi_N = \frac{\pi}{6}$) and not at the maxima of the input currents (for $\varphi_N \in [0, \frac{\pi}{6}]$ the maximum mains current occurs for $\varphi_N = 0$ in phase R). Under consideration of Eq.(7) and Eq.(8) we have:

$$\delta = \delta_P\,\frac{M}{M - 1}. \tag{15}$$

For $\delta = 1$ that duty ratio is defined by Eq.(15) for a given M for which the
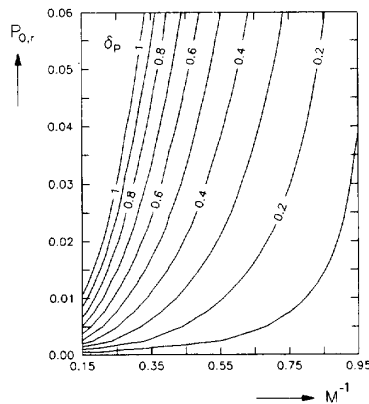
limit to the discontinuous mode is reached. Regarding a system dimensioning one has to raise the question now to which output power this duty ratio corresponds. Due to the constant output voltage the output power is determined directly by the (global) mean value $I_{D,avg}$ of the diode current i_D. This can be seen clearly from the expression:

$$P_{O,r} \equiv I_{D,avg,r}. \tag{16}$$

Based on Eq.(1) one can calculate the output power directly in analytically closed form, therefore. After an extensive calculation there follows:

$$P_{O,r} = \frac{1}{2}\delta_P^2\left[\frac{3}{\pi}\left(\frac{M}{\sqrt{M^2 - 3}}(\tan^{-1}\frac{\sqrt{3}}{\sqrt{M^2 - 3}} + \tan^{-1}\frac{\frac{\sqrt{3}-1}{\sqrt{3}+1}M - \sqrt{3}}{\sqrt{M^2 - 3}})\right.\right.$$
$$\left.\left. + \frac{3M}{\sqrt{M^2 - 1}}\tan^{-1}\frac{\sqrt{3}-1}{\sqrt{3}+1}\sqrt{\frac{M + 1}{M - 1}} - \frac{\sqrt{3}}{2}M^{-1}\right) - 1\right] \tag{17}$$

(cf. **Fig.5**). By combining of Eqs.(15,17) one can now determine the limit of the discontinuous mode in relation to the converter output power. The resulting relation is shown in **Fig.6**. The power which can be supplied for $\delta = 1$ is essentially determined by the value of the voltage transfer ratio. For an input voltage being small as compared to the output voltage (small values of M^{-1}) the magnetization interval ($t_\mu \in [0, t_{\mu,1}]$) is pronounced in the current shape; for high input voltage ($M^{-1} \approx 1$) due to the low voltage difference the demagnetization interval ($t_\mu \in [t_{\mu,1}, t_{\mu,3}]$) is very pronounced. In both cases only relatively low current values $i_{i,t\mu1}$ and low output power values are obtained. An optimum utilization of the pulse period and, therefore, high output power, is given only for $M^{-1} \approx 0.5$ or $\sqrt{3}\hat{U}_N \approx \frac{1}{2}U_O$, respectively.

For the calculation of the fundamental of the mains current which defines the output power of the converter we use the balance of power:

$$P_O = U_O I_O = U_O I_{D,avg} = \frac{3}{2}\hat{U}_N \hat{I}_{N,(1)}. \tag{18}$$

There, loss-free operation is assumed (cf. sections 3.1). With section 3.3 and with Eqs.(6,16) there follows:

$$\hat{I}_{N,(1),r} = \frac{2}{\sqrt{3}}M\,P_{O,r}. \tag{19}$$
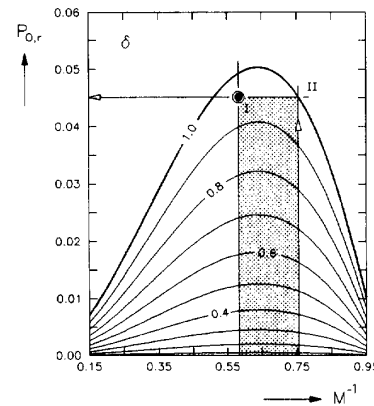
5 Component Ratings

For a dimensioning and for an assessment of the application region of the system especially the current and voltage stresses on the power electronic devices as well as on the passive components are of interest.

5.1 Blocking Voltage Stress on the Power Semiconductors

As Fig.2 shows clearly, the ideal maximum blocking voltage stress on all power electronic devices is defined by the output voltage. We have:

$$U_{T,max} = U_{D,max} = U_{Di,max} = U_O. \tag{20}$$

5.2 Maximum Values, Average Values and RMS Values of the Device Currents

Fig.5: Dependency of the rated output power $P_{O,r}$ on the duty cycle δ_P of T and on the voltage transfer ratio M (cf. Eq.(17)).

Fig.6: Dependency of $P_{O,r}$ on the rated maximum conduction interval δ of the diode bridge and on M; $\delta = 1$ defines the limit between continuous and discontinuous mode; validity of the representation limited to discontinuous mode ($\delta \leq 1$) as for all other results given in this paper. The operating region resulting for the dimensioning example given in section 7.2 is marked.

The (global) mean and rms values of the device currents are calculated based on section 4 by using the defining equations Eqs.(1,2). E.g., there follows for the characteristic parameters of the transistor current:

$$I_{T,avg,r} = \frac{3\sqrt{3}}{4\pi} M^{-1} \delta_P^2 , \tag{21}$$

$$I_{T,rms,r}^2 = \left(\frac{1}{8} + \frac{3\sqrt{3}}{16\pi}\right) M^{-2} \delta_P^3 . \tag{22}$$

For $t_\mu \le t_{\mu,1}$ and the angle interval $\varphi_N \in [0, \frac{\pi}{6}]$ the local shape of the transistor current i_T is identical to the shape of $i_{U,R}$. The global maximum value within the fundamental period therefore is given via Eq.(10):

$$I_{T,max,r} = \frac{\sqrt{3}}{2} M^{-1} \delta_P . \tag{23}$$

The characteristic quantities given can now (with the application of Eq.(17)) again be brought into a direct relation to the output power (as shown in section 4 for the example of the quantity δ, cf. Fig.6). The resulting dependencies are shown in **Fig.7**, (a)–(c). There, the limit of the discontinuous mode is shown as characteristic curve $\delta = 1$. The characteristic transistor current quantities being related to a given output power are thereby defined in the entire input and output voltage region (being of interest for a practical realisation). Therefore, a fast and simple dimensioning is made possible.

For the sake of brevity, the further discussion is limited to a few basic issues. A description of the relatively involved calculation of further component stresses being relevant for dimensioning is omitted. The calculated rms values of the device currents are compiled in Fig.7 (d)–(h). The characteristic values of the currents not shown in Fig.7 can be determined easily by the relations given in the following.

The maximum current stress on the input inductances L_U, on the diodes of the three-phase bridge and on the output diode is given (according to the operating principle of the system) by the global maximum value of the transistor current:

$$I_{T,max,r} = I_{D,max,r} = I_{U,(RST),max,r} = I_{Di,max,r} . \tag{24}$$

Therefore, it can be directly read from Fig.7, (c).

Due to the constant output current and due to the average value of the current through the output capacitor being zero one can use the relation

$$I_{C,rms,r}^2 = I_{D,rms,r}^2 - I_{O,r}^2 \tag{25}$$

for determining $I_{C,rms}$ (cf. Fig.7, (d) and Eq.(18)). For pulsating output current i_O we have to use

$$I_{C,rms,r} = I_{D,rms,r} + I_{O,rms,r} \tag{26}$$

in order to give a worst-case estimate [9]. An estimate of the noise voltage level (with switching frequency) on the output side can be given via the global maximum value

$$I_{C,max,r} = I_{D,max,r} - I_{O,r} \tag{27}$$

and by the ESR of the output capacitor.

Based on the assumption of ideal filtering of the switching frequency spectral components of the converter input currents $i_{U,(RST)}$ one can set for the AC side converter quantities (in analogy to Eq.(25))

$$I_{CN,rms,r}^2 = I_{U,rms,r}^2 - I_{N,rms,r}^2 . \tag{28}$$

For multi-stage filtering of the converter currents, C_N denotes the output capacitor of the mains filter. The low-frequency component of the capacitor current

$$I_{CN,rms,(1)} = \omega_N C_N U_{N,rms} \tag{29}$$

(not being represented in Eq.(28)) can be neglected in most cases, as compared to the switching frequency component stress. For the global maximum value of the capacitor current there follows approximately:

$$I_{CN,max,r} = I_{U,(RST),max,r} - \hat{I}_{N,(1),r} . \tag{30}$$

Remark: As discussed in connection with Eq.(28), the rms value $I_{CN,rms}$ is generated by the harmonics (with switching frequency) of an input phase current $i_{U,i}$. Therefore, $I_{CN,rms}$ makes possible (besides the determination of the current stress on the mains filter capacitor) also an estimate of that part of the resistive losses in a phase inductance L_U which is caused by the current harmonics. There, due to the skin and proximity effects, the DC current resistance of the winding has to be increased by a factor given by the switching frequency and the cross-section of the wire (or penetration depth,

respectively). For calculating the overall resistive losses one has to add to this loss contribution that loss which is caused by the low-frequency harmonics of $i_{U,i}$, which is described via $I_{N,rms}$ and which is calculated based on the DC resistance [10].

For the characteristic quantities of the diodes $D_{i=1...6}$ of the three-phase bridge we have (as can be seen directly from the operating principle of the circuit):

$$I_{Di,avg,r} = \frac{1}{3}(I_{T,avg,r} + I_{D,avg,r}) , \tag{31}$$

$$I_{Di,rms,r} = \frac{1}{\sqrt{2}} I_{U,rms,r} . \tag{32}$$

5.3 Conduction and Switching Losses of the Power Semiconductors

The calculation of the conduction losses of the power semiconductors can be performed advantageously by approximating the on-state voltage drop by

$$u_{F,i} = U_{F,i} + r_{F,i} i_i \tag{33}$$

(cf., [5]). Therefore, for the conduction losses there follows in general:

$$P_{F,i} = U_{F,i} I_{i,avg} + r_{F,i} I_{i,rms}^2 . \tag{34}$$

Concerning the switching losses especially the stress on the power transistor is of importance for dimensioning. As shown in the following, this stress can be also calculated by a simple analytical relation.

Due to the discontinuous mode of the converter the turn-on losses can be neglected as compared to the turn-off losses. Based on a linear relation (as first approximation) of the power loss occurring during the turn-off process

$$w_{P,T} = k_T i_T \qquad [k_T] = \frac{Ws}{A} , \tag{35}$$

a local switching power loss

$$p_{P,T} = \frac{1}{T_P} w_{P,T} \tag{36}$$

is defined by averaging over a pulse period. Averaging of $p_{P,T}$ within the interval $\varphi \in [0, \frac{\pi}{6}]$ leads to the switching losses being proportional to the global peak value of the transistor current:

$$P_{P,T} = \frac{2}{\pi} \frac{k_T U_O}{L_U} I_{T,max,r} . \tag{37}$$

6 Mains Current

For the calculation of the fundamental component and the low-frequency harmonic components of the mains currents (remaining after filtering of the switching frequency components of the diode bridge input currents) local averaging can be used [8]. Based on symmetry considerations one can extend the description of the phase currents within the fundamental section $\varphi_N \in [0, \frac{\pi}{6}]$ to the interval $\varphi_N \in [0, \frac{\pi}{2}]$. For the shape of the mains current there follows (phase R):

Interval $[0, \frac{\pi}{6}]$:

$$i_{N,R,r}(\varphi_N) = \frac{\sqrt{3}}{4} \delta_P^2 M^{-1} \frac{\cos(\varphi_N) - 2M^{-1}\cos(\varphi_N)\cos(\varphi_N + \frac{\pi}{6}) + \frac{\sqrt{3}}{2}M^{-1}}{\left(1 + \sqrt{3}M^{-1}\sin(\varphi_N - \frac{\pi}{6})\right)\left(1 - M^{-1}\cos(\varphi_N - \frac{\pi}{6})\right)} \tag{38}$$

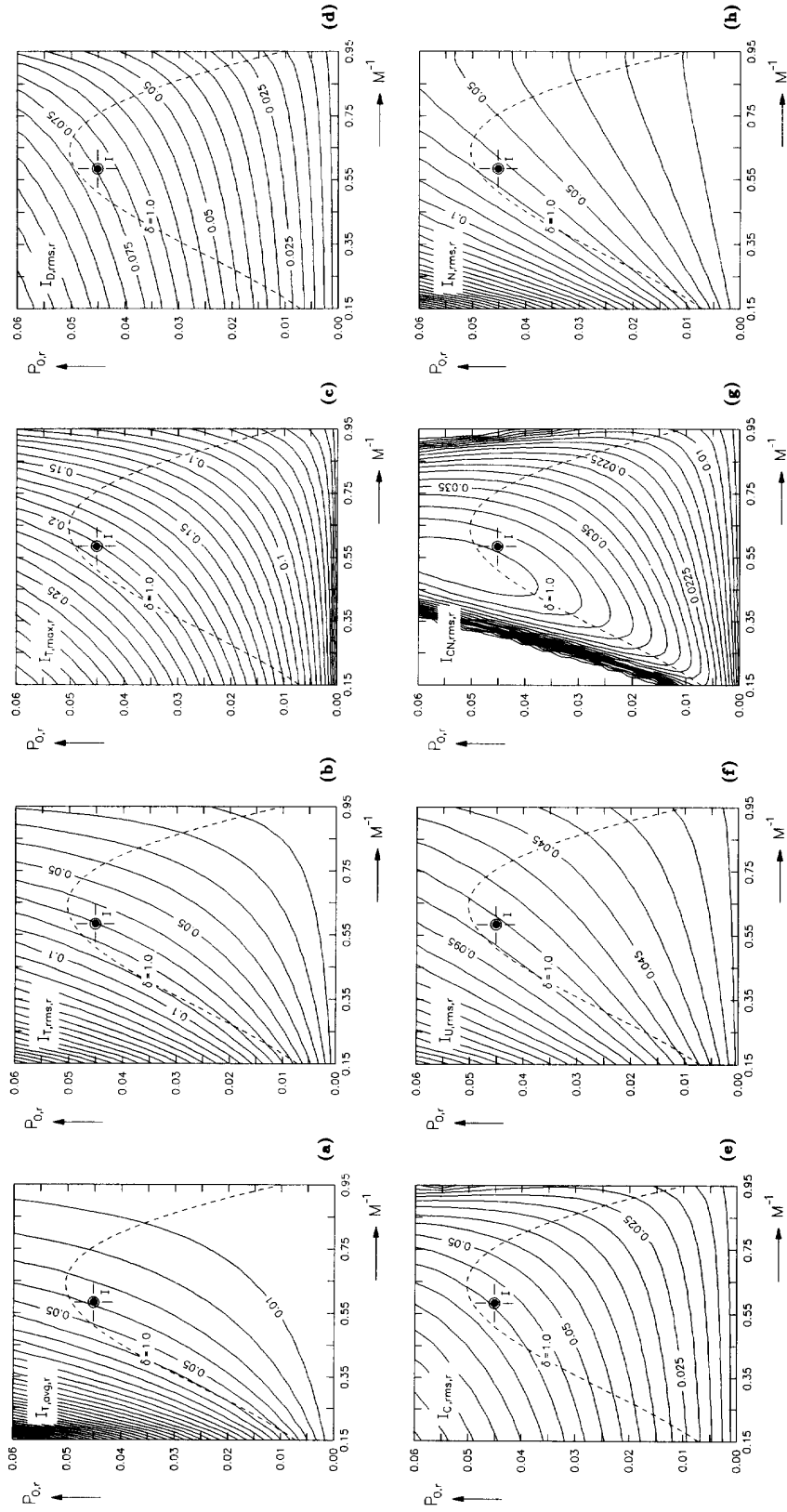Interval $[\frac{\pi}{6}, \frac{\pi}{3}]$:

$$i_{N,R,r}(\varphi_N) = \frac{\sqrt{3}}{4} \delta_P^2 M^{-1} \frac{\cos(\varphi_N) + \frac{1}{2}M^{-1}\cos(2\varphi_N + \frac{\pi}{6})}{\left(1 - \sqrt{3}M^{-1}\sin(\varphi_N - \frac{\pi}{6})\right)\left(1 - M^{-1}\cos(\varphi_N - \frac{\pi}{6})\right)} \tag{39}$$

Interval $[\frac{\pi}{3}, \frac{\pi}{2}]$:

$$i_{N,R,r}(\varphi_N) = \frac{\sqrt{3}}{4} \delta_P^2 M^{-1} \frac{\cos(\varphi_N)}{1 - \sqrt{3}M^{-1}\cos(\varphi_N)} . \tag{40}$$

Based on the analytical description given here one can now directly calculate the mains current harmonics which are of interest for an assessment of the effects on the mains (cf. **Fig.8**). For calculating the power factor we have to apply

$$\lambda = \frac{I_{N,(1),rms}}{I_{N,rms}} \tag{41}$$

935

Fig.7: Dependencies of the rated characteristic current quantities characterizing the component stresses on the rated output power $P_{O,r}$ and on the voltage transfer ratio M; the validity of the diagrams is limited to the discontinuous mode (the limit between continuous and discontinuous mode is shown as characteristic curve $\delta = 1$ (cf. Fig.6)); (a): average value of the transistor current; (b): rms value of the transistor current; (c): peak value of the transistor current; (d): rms value of the output diode current; (e): rms value of the output capacitor current; (f): rms value of the converter input current; (g): rms value of the mains filter capacitor current; (h): rms value of the mains current. The operating point $M_{max} = 1.71$, $P_{O,r,\delta \leq 1} = 0.045$ (cf. I in Fig.6), which is used in section 7.2 for the design example for determining the maximum component stress, is marked.
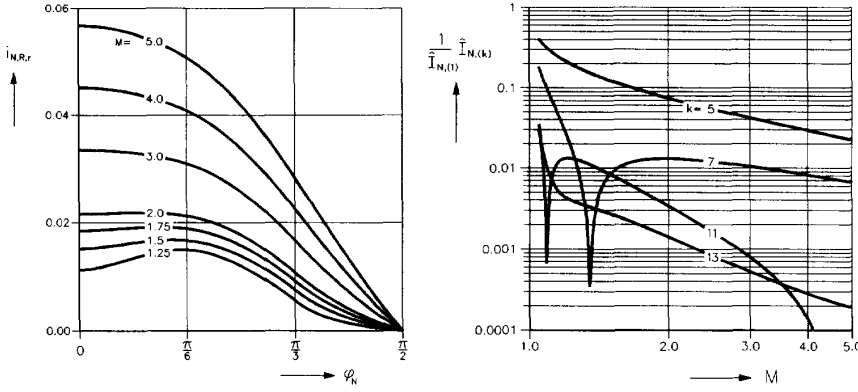
Fig.8: Representation of the analytically calculated time shapes (shown for a quarter fundamental period) and of the low-frequency mains current harmonics $\hat{I}_{N,(k)}$ (related to the fundamental $\hat{I}_{N,(1)}$) in dependency on the voltage transfer ratio M; constant pulse frequency f_P and constant on-time $t_{\mu,1}$ of the power transistor T within the fundamental period; parameter: $P_{O,r} = 0.01$.

due to the purely sinusoidal, symmetric mains voltage system. There, the current fundamental is assumed as being in phase with the mains voltage. The phase shift between mains voltage and mains current caused by the input filter is not considered due to the assumed essential higher cut-off frequency of the filter as compared to the mains frequency.

As **Fig.9** shows, the effects on the mains as caused by the converter are influenced essentially in the region $M < 1.2$ by the voltage transfer ratio. For $M < 1.09$ the power factor falls to values $\lambda < 0.95$, due to the occurrence of low-frequency harmonics in the mains current spectrum. A power factor > 0.98 ($\hat{I}_{N,(5)} < 0.2\hat{I}_{N,(1)}$) is obtained only for $U_O > 3U_{N,rms}$ ($M > 1.22$). For operating the converter from the European low-voltage mains this means a relatively high output voltage ($U_O > 760$ V, where the mains voltage tolerance band is considered), considering today's typical maximum allowed blocking voltage (about 1200 V) of high-voltage power transistors.

7 Converter Design

As shown in the following, the calculation results being represented in rated form allow a direct and simple dimensioning of the system components.

7.1 Design Procedure

The main point of the dimensioning is the calculation of that value of the inductance L_U which guarantees the discontinuous mode in the entire input voltage and output power region for maximum utilisation of the pulse interval (and, therefore, of the rated power of the converter). The maximum output power $P_{O,max}$, the controlled output voltage U_O and the input voltage region $\hat{U}_N \in [\hat{U}_{N,min}, \hat{U}_{N,max}]$ may be given.

The global maximum value of the rated conduction interval δ (which has to be considered for dimensioning) is set, as explained in section 4, by the voltage transfer ratio and by the rated output power. Using the dependency (shown graphically in Fig.6) one can now determine that power value

$$P_{O,r,\delta\leq1} = \min\left\{P_{O,r}(M^{-1},\delta)\right\}_{M^{-1}\in[M_{min}^{-1},M_{max}^{-1}],\ \delta=1} \qquad (42)$$
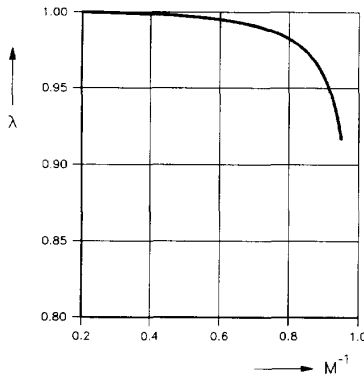

Fig.9: Mains power factor (cf. Eq.(41)) in dependency on the voltage transfer ratio M.

for which the system operates in the entire input voltage region in the discontinuous mode ($\delta \leq 1$). By inversion of the normalization equation of the power (cf. Eq.(4)) one can calculate the critical value of the inductance as:

$$L_U \leq \frac{2}{3}U_O^2 T_P \frac{P_{O,r,\delta\leq1}}{P_{O,max}} . \qquad (43)$$

The operating region of the system is described by a rectangle defined by the intervals $P_{O,r} = [0, P_{O,r,\delta\leq1}]$, $M^{-1} \in [M_{min}^{-1}, M_{max}^{-1}]$ in the $P_{O,r}, M^{-1}$-plane. For determination of the maximum current stress on the devices, one can now assume this rectangle to be inserted into Fig.7. Then, the maximum occurring component stresses can be seen immediately or can be calculated via Eq.(27), Eq.(30), Eq.(31) and Eq.(32).

7.2 Design Example

We assume:

$$\begin{aligned}
U_{N,rms} &= 230\,\text{V}_{-15\%}^{+10\%} \\
P_O &= 7.5\,\text{kW} \\
U_O &= 820\,\text{V} \\
f_P &= 48\,\text{kHz} \quad (T_P = 20.8\mu s) .
\end{aligned}$$

Because we have assumed a loss-free system for easier calculation (cf. section 3.1), we have to increase the output power for system dimensioning as compared to the actual output power by the system losses as a first approximation. For a sufficient safe dimensioning we estimate a converter efficiency of $\eta \approx 0.9$. Therefore, the basis for dimensioning will be $P_{O,max} = 8300\,\text{W}$. For the voltage transfer ratios for minimum and maximum input voltage there follows with Eq.(6):

$$\begin{aligned}
M_{max} &= 1.71 \quad (U_{N,rms,min} = 195.5\,\text{V}) \\
M_{min} &= 1.32 \quad (U_{N,rms,max} = 253.0\,\text{V}) .
\end{aligned}$$

For the sake of clearness the consideration of a control margin shall be omitted for the calculation of the inductance L_U. The dimensioning shall be performed such that for $P_O = P_{O,max}$ the limit of the discontinuous mode $\delta = 1$ is reached. In order to guarantee $\delta \leq 1$ in the entire input voltage region, we have to choose

$$P_{O,r,\delta\leq1} = 0.045 ,$$

according to Fig.6. Here, $\delta = 1$ is reached for M_{min} (cf. II in Fig.6). With this and with Eq.(43) there follows the dimensioning of the input inductances:

$$L_U = 50.6\,\mu\text{H} .$$

For the relative on-time of the power transistor for minimum and maximum input voltage there follows with Eq.(17) or with Fig.5:

$$\begin{aligned}
\delta_{P,max} &= 0.39 \\
\delta_{P,min} &= 0.24 .
\end{aligned}$$

As discussed in section 5.1, the ideally maximum blocking voltage stress on the power semiconductors

$$U_{T,max} = U_{D,max} = U_{Di,max} = 820 \text{ V}$$

is defined by the output voltage, where for the setting of the blocking voltage capability of the devices transient switching and mains overvoltages have to be considered.

937

For determining the maximum current stress on the devices we have to transfer the operating point I (cf. Fig.6) as given for minimum input voltage $\hat{U}_{N,rms,min}$ (or M_{max}, respectively) and for maximum output power $P_{O,max}$ (or $P_{O,r,\delta\le1}$, respectively) into the diagrams of Fig.7. Then, the maximum component stress can be read directly and/or be calculated via the relations given in section 5.

With the normalization basis for the current values

$$I_n = 225.1\,\text{A}$$

(cf. Eq.(5)) there follows:

Power transistor T:

$$\text{Fig.7,(a)} : I_{T,avg} = 8.6\,\text{A}$$
$$\text{Fig.7,(b)} : I_{T,rms} = 16.0\,\text{A}$$
$$\text{Fig.7,(c)} : I_{T,max} = 45.5\,\text{A}$$

Inductance L_U:

$$\text{Fig.7,(f)} : I_{U,(RST),rms} = 17.5\,\text{A}$$
$$\text{Eq.(24)} : I_{U,(RST),max} = 45.5\,\text{A}$$

Output diode D:

$$\text{Eq.(18)} : I_{D,avg} = 10.1\,\text{A}$$
$$\text{Fig.7,(d)} : I_{D,rms} = 16.6\,\text{A}$$
$$\text{Eq.(24)} : I_{D,max} = 45.5\,\text{A}$$

Diodes D_i of the three-phase bridge:

$$\text{Eq.(31)} : I_{Di,avg} = 6.2\,\text{A}$$
$$\text{Eq.(32)} : I_{Di,rms} = 12.5\,\text{A}$$
$$\text{Eq.(24)} : I_{Di,max} = 45.5\,\text{A}$$

Output capacitor C:

$$\text{Fig.7,(e)} : I_{C,rms} = 13.2\,\text{A}$$
$$\text{Eq.(27)} : I_{C,max} = 35.4\,\text{A}$$

Mains filter capacitor C_N:

$$\text{Fig.7,(g)} : I_{CN,rms} = 10.0\,\text{A}$$
$$\text{Eq.(30)} : I_{CN,max} = 25.5\,\text{A} .$$

Remark: According to Eq.(5) the reference values I_n and P_n of the normalization remain unchanged for proportional change of pulse frequency $f_P = T_P^{-1}$ and inductivity L_U. If now f_P is changed during dimensioning and L_U is adjusted accordingly, the current stress on the devices is *not* influenced and can be taken directly from the original dimensioning.

For the output current there follows with Eq.(16) and Eq.(18)):

$$I_O = 10.1\,\text{A} .$$

Characteristic values of the mains current:

$$\text{Eq.(19)} : \hat{I}_{N,(1)} = 20.0\,\text{A}$$
$$\text{Fig.7,(h)} : I_{N,rms} = 14.4\,\text{A} .$$

The maximum amplitudes of the low-frequency mains current harmonics can be taken from Fig.8 for M_{min}, the minimum power factor from Fig.9. The maximum amplitude of the 5th harmonic is of special importance regarding the effects on the mains. There follows:

$$\frac{\hat{I}_{N,(5),max}}{\hat{I}_{N,(1)}} = 0.16 .$$

Therefore, for the maximum input voltage a considerable deviation of the mains current from an ideally purely sinusoidal shape occurs. This shows up also in the value of the power factor:

$$\lambda_{min} = 0.985 .$$

8 Conclusions

In this paper a procedure is introduced which can be applied in a simple way for determining the component stresses in a three-phase single-switch DICM boost rectifier system. Because the mathematical modelling avoids an application of a single-phase equivalent system, the derived relations show

an excellent consistency with the results of a digital simulation also for low values of the voltage transfer ratio (e.g., $U_O = 820$ V, $M \approx 1.5$, as being of interest for a practical application in the European low-voltage system with a line-to-line voltage $\sqrt{3}\hat{U}_N = 380$ V). The deviation of the calculated results remains below 2% for pulse frequencies $f_P \ge 200 f_N$. We have to point out finally that the calculation results can be used also for dimensioning of the devices of the input circuit and for the analysis of the mains behavior of other three-phase single-switch DICM rectifiers with equal structure of the input circuit (cf. [11], [12]). Therefore, the analysis given is valid for a whole class of converter structures.

References

[1] **Bose, B.K.**: *Recent Advances in Power Electronics*. IEEE Transactions on PE, Vol.7, No.1, pp. 2–16 (1992).

[2] **Zhang, H.**: *Reversible Rectifiers*. Ph.D Thesis, University of Surrey, Guildford, England, (1992).

[3] **Koczara, W.**: *Unity Power Factor Three-Phase Rectifier*. Proceedings of 6th International (2nd European) Power Quality Conference, Oct. 14–15, Munich, pp. 79–88 (1992).

[4] **Prasad, A.R., Ziogas, D., and Manias, S.**: *An Active Power Factor Correction Technique for Three-Phase Diode Rectifiers*. IEEE Transactions on PE, Vol.6, No.1, pp. 83–92 (1991).

[5] **Kolar, J.W., Ertl, H., and Zach, F.C.**: *Calculation of the Passive and Active Component Stress of Three-Phase PWM Converter Systems with High Pulse Rate*. Proceedings of the 3rd European Conference on Power Electronics and Applications, Aachen, Oct. 9–12, Vol.3, pp.1303–1311 (1989).

[6] **Redl, R., and Balogh, L.**: *RMS, DC, Peak, and High-Frequency Power-Factor Correctors with Capacitive Energy Storage*. Proceedings of the 7th Applied Power Electronics Conference, Boston, MA, Feb. 23–27, 533–540 (1992).

[7] **Malesani, L., Rossetto, L., Spiazzi, G., Tenti, P., Toigo, I., and Dal Lago, F.**: *Single-Switch Three-Phase AC-DC Converter with High Power Factor and Wide Regulation Capability*. Proceedings of the 14th International Telecommunications Energy Conference, Washington, D.C., Oct. 4–8, pp. 279–285 (1992).

[8] **Kolar, J.W., Ertl, H., and Zach, F.C.**: *Space Vector - Based Analytical Analysis of the Input Current Distortion of a Three-Phase Discontinuous-Mode Boost Rectifier System*. Record of the 24th IEEE Power Electronics Specialists Conference, Seattle, June 20–24 (1993).

[9] **Kolar, J.W., Ertl, H., and Zach, F.C.**: *Approximate Determination of the Current RMS Value of the DC Link Capacitor of Single-Phase and Three-Phase PWM Converter Systems*. Proceedings of the 3rd International (1st European) Power Quality Conference, Paris, Nov. 13–15 (1990).

[10] **Dixon Jr., L.H.**: *Filter Inductor and Flyback Transformer Design for Switching Power Supplies*. Unitrode Switching Regulated Power Supply Design Seminar Manual, SEM-700, pp. M6-1–M6-6 (1990).

[11] **Ismail, E., and Erickson, R.W.**: *A Single Transistor Three-Phase Resonant Switch for High-Quality Rectification*. Conference Record of the 23rd Power Electronics Specialists Conference, Madrid, June 29–July 3, Vol.II, pp. 1341–1351 (1992).

[12] **Kolar, J.W., Ertl, H., and Zach, F.C.**: *Power Quality Improvement of Three-Phase AC-DC Power Conversion by Discontinuous Mode 'Dither'-Rectifiers*. Proceedings of 6th International (2nd European) Power Quality Conference, Oct. 14–15, Munich, pp. 62–78 (1992).